Environ. Sci. Technol. **2004**, *38,* 2058−2066

Mechanisms and Products of Surface-Mediated Reductive Dehalogenation of Carbon Tetrachloride by Fe(II) on Goethite

MARTIN ELSNER,[†]
STEFAN B. HADERLEIN,[‡]
THOMAS KELLERHALS, SAMUEL LUZI,
LUC ZWANK, WERNER ANGST, AND
RENÉ P. SCHWARZENBACH*
Swiss Federal Institute of Environmental Science and
Technology (EAWAG), Ueberlandstrasse 133,
CH-8600 Duebendorf

Natural attenuation processes of chlorinated solvents in soils and groundwaters are increasingly considered as options to manage contaminated sites. Under anoxic conditions, reactions with ferrous iron sorbed at iron(hyro)-xides may dominate the overall transformation of carbon tetrachloride (CCl_4) and other chlorinated aliphatic hydrocarbons. We investigated mechanisms and product formation of CCl_4 reduction by Fe(II) sorbed to goethite, which may lead to completely dehalogenated products or to chloroform ($CHCl_3$), a toxic product which is fairly persistent under anoxic conditions. A simultaneous transfer of two electrons and cleavage of two C−Cl bonds of CCl_4 would completely circumvent chloroform production. To distinguish between initial one- or two-bond cleavage, ^{13}C-isotope fractionation of CCl_4 was studied for reactions with Fe(II)/goethite (isotopic enrichment factor $\epsilon = -26.5‰$) and with model systems for one C−Cl bond cleavage and either single-electron transfer (Fe(II) porphyrin, $\epsilon = -26.1‰$) or partial two-electron transfer (polysulfide, $\epsilon = -22.2‰$). These ϵ values differ significantly from calculations for simultaneous cleavage of two C−Cl bonds ($\epsilon \approx -50‰$), indicating that only one C−Cl bond is broken in the critical first step of the reaction. At pH 7, reduction of CCl_4 by Fe(II)/goethite produced ∼33% $CHCl_3$, 20% carbon monoxide (CO), and up to 40% formate ($HCOO^-$). Addition of 2-propanol-d_8 resulted in 33% $CDCl_3$ and only 4% CO, indicating that both products were generated from trichloromethyl radicals ($^{\bullet}CCl_3$), chloroform by reaction with hydrogen radical donors and CO by an alternative pathway likely to involve surface-bound intermediates. Hydrolysis of CO to $HCOO^-$ was surface-catalyzed by goethite but was too slow to account for the measured formate concentrations. Chloroform yields slightly increased with pH at constant Fe(II) sorption density, suggesting that pH-dependent surface processes direct product branching ratios. Surface-stabilized intermediates may thus facilitate abiotic mineralization of CCl_4, whereas the presence of H radical donors, such as natural organic matter, enhances formation of toxic $CHCl_3$.

Introduction

Aliphatic chlorinated hydrocarbons, including carbon tetrachloride (CCl_4), are widespread groundwater contaminants (*1−4*). While such compounds are rather persistent under oxic conditions, they may undergo reductive dehalogenation under reducing conditions in the subsurface. Depending on the predominating environmental conditions, dehalogenation of CCl_4 can lead to harmless end products, but can also lead to more persistent compounds. The majority of studies on abiotic reductive dehalogenation of CCl_4 reported hydrogenolysis to chloroform ($CHCl_3$), which is toxic and more recalcitrant than CCl_4 under anoxic conditions. Most studies, however, also report incomplete mass balances (*5,6*) or partial conversion of CCl_4 to completely dehalogenated products that are indicative of alternative dehalogenation pathways of CCl_4 (*7−14*). Formate ($HCOO^-$), carbon monoxide (CO), and carbon dioxide (CO_2) were found during electrolytic dehalogenation of CCl_4 at a silver electrode (*7*); formate in the reaction of CCl_4 with goethite/Fe(II) (*8*); and CO and CO_2 in the reaction with pyrite or with sulfide in the presence of layer silicates (*9,10*) as well as in photochemical transformation of CCl_4 in water (ice) films (*11*). Transformation of CCl_4 by *Pseudomonas stutzeri* KC is the only case of biotransformation in which readily degradable (thio)phosgene ($S{=}CCl_2/O{=}CCl_2$) and CO_2 accounted for most of the mass balance, and only traces of $CHCl_3$ were found (*12,13*). Other microorganisms studied produced $CHCl_3$ as a major product (*14*). Therefore, hydrogenolysis and complete dehalogenation are concurrent and, thus, competing pathways in the dehalogenation of CCl_4 by various reductants, and knowledge about the conditions that favor either pathway is of great interest, both for evaluation of natural attentuation and for the design of remediation schemes.

Reduction of CCl_4 is believed to start in most cases with a single electron transfer and simultaneous cleavage of one C−Cl bond, which leads to short-lived trichloromethyl radicals (single-electron-transfer, Scheme 1).

SCHEME 1

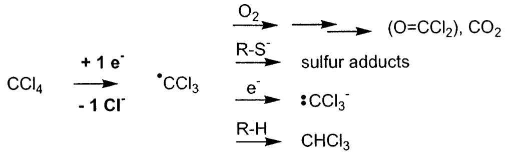

In such a case, product formation is determined by radical reactions of $^{\bullet}CCl_3$ with system components. Presence of molecular oxygen, for example, causes reoxidation to phosgene/CO_2 (*11,15*); sulfide creates sulfur adducts (*9,10,16*); transfer of a second electron causes further reduction; and $H^{\bullet}$ radical donors, such as organic compounds, favor $CHCl_3$ formation (*13,16,17*). Alternatively, a concerted transfer of *two* electrons with simultaneous cleavage of *one* C−Cl bond is believed to take place in a nucleophilic attack of strong reductants at the halogen center (X-philic reactions, Scheme 2) (*16,18*), thus leading directly to short-lived trichloromethyl anion intermediates.

In such a case, the product formation is governed by the rate of H^+ transfer relative to that of self-decomposition of CCl_3^- (*19*). Proton transfer leads to chloroform. Loss of Cl^-

---

* Corresponding author phone: (++41 1) 823 5109; fax: (++41 1) 823 5471, e-mail: schwaba@eawag.ch.

[†] Present address: Department of Geology, University of Toronto, 22 Russell Street, Toronto, Ontario M5S 3B1.

[‡] Present address: Center for Applied Geosciences (ZAG), Eberhard-Karls University, Wilhelmstr. 56, D-72074 Tuebingen.

10.1021/es034741m CCC: $27.50

SCHEME 2

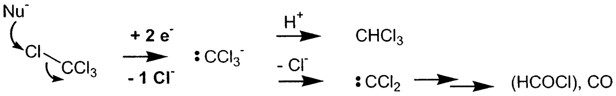

from CCl_3^- yields dichlorocarbene, which rapidly hydrolyses to formyl chloride (HCOCl) (*20*) and, eventually, to CO (*21*). Because both Scheme 1 and Scheme 2 can lead to $CHCl_3$, it is intrinsically impossible to circumvent chloroform production, except for a theoretical third case in which *two* electrons are transferred and simultaneously, *two* C−Cl bonds are broken in the initial reaction step so that dichlorocarbene is formed directly (*8*) (case 3, Scheme 3).

SCHEME 3

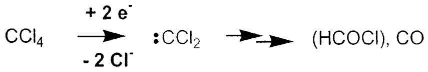

Simultaneous cleavage of two C−Cl bonds, however, is highly endergonic, whereas the postulate of transition state theory requires that the reaction coordinate proceeds along a path of lowest activation energy. In solution, that is, without stabilization of the respective intermediate(s), generally only one C−Cl bond will thus be initially broken; the situation, however, may be different on surfaces, where a transition state of the type ═S- - -Cl- - -CCl_2- - -Cl- - -S═ can be imagined that may reduce the activation energy for simultaneous cleavage of two bonds (where ═S denotes surface groups).

Because of the great importance and ubiquitous occurrence of ferrous iron sorbed at natural mineral surfaces, we focus in this study on elucidating the pathways of reductive dehalogenation of CCl_4 by reactive surface-bound Fe(II) species. McCormick et al. (*22*) reported that reductive dehalogenation of CCl_4 in the presence of iron-reducing bacteria was mainly due to abiotic reaction with Fe(II) at the surface of biogenic magnetite and only to a small extent to direct enzymatic dehalogenation. In many other studies, Fe(II) sorbed to mineral surfaces was found to be by orders of magnitude more reactive than Fe(II) in solution (*23*−*26*). It has been found that for some contaminants including CCl_4, reactions with Fe(II) sorbed at iron(hyro)xides may be the dominating removal process under anoxic conditions (*27*,*28*). Surface-bound Fe(II) is also thought to play a role in metal iron reactive walls that are increasingly used to clean up contaminated aquifers (*29*).

Pecher et al. (*8*) identified chloroform and formate as major products of the reaction of CCl_4 with Fe(II) sorbed to goethite at circumneutral pH and found increasing yields of $CHCl_3$ with higher pH. Amonette et al. (*6*) obtained in similar systems under acidic conditions a rate law that was second-order with respect to sorbed Fe(II) and first-order with respect to dissolved CCl_4. They postulated a termolecular initial two-electron reaction step in which each of two adjacent Fe(II) surface sites conveyed simultaneously one electron to a CCl_4 molecule.

To date, the reaction mechanisms and conditions that cause formation of toxic chloroform vs completely dehalogenated products are not well-understood for this reaction. In particular, it remains unclear whether and under which conditions a simultaneous two-electron transfer associated with a two-bond-cleavage process can occur and whether formation of chloroform may be attributable to an initial single-electron transfer or, alternatively, generation of formate to an initial two-electron transfer. The objectives of this study were, therefore, (i) to complete the mass balance of the reductive dehalogenation of CCl_4 by goethite/Fe(II) and to investigate how environmental conditions (pH, Fe(II) surface site coverage, presence of $^\bullet$H donors) influence product formation (i.e., chloroform, formate, and potentially other products); and (ii) to gain more insight into the mechanism of product formation on the basis of information from product studies and trapping experiments, as well as from a complementary isotope fractionation study.

To distinguish between initial one- and two-bond-cleavage processes, ^{13}C-isotope fractionation during dehalogenation of CCl_4 was studied with various electron donors. Completion of mass balances was attempted by comprehensive analyses of reaction products at pH 7, including CO, $CHCl_3$, and formate. To trap intermediate $^\bullet CCl_3$ radicals, an efficient $D^\bullet$ radical donor (perdeuterated 2-propanol) was used, or alternatively, great care was taken to exclude possible $H^\bullet$ radical donors from the experimental system such as organic buffers (e.g., MOPS, HEPES). To distinguish the influence of pH from that of Fe(II) surface site coverage, experiments were conducted at different pHs, but constant Fe(II) sorption site density.

Materials and Methods

Great care was taken in experiments with goethite/Fe(II) to minimize organic residues which could serve as possible H radical donors in the experimental system. Prior to the experiments, the goethite was repeatedly washed with deionized water to remove organic acids known to be present at the surface (*30*,*31*). Moreover, organic ("Goods") buffers were avoided, since they are known to transfer $H^\bullet$ atoms to $^\bullet CCl_3$ radicals and, thus, generate chloroform [see Scheme 1 (*13*)]. Instead, pH control was ensured by the intrinsic buffer effect of ═S−O−Fe(II)−OH groups at the goethite surface. This buffer capacity was examined for representative experimental conditions (50 m^2/L goethite in equilibrium with 1 mM dissolved $Fe(II)_{aq}$) by acid/base titrations between pH 7 and 8. The determined buffer intensity was 250−300 μM per pH unit, meaning that 250−300 μM acid/base had to be added in order to change the pH value by one unit. Calculations showed that this was sufficient to ensure pH control during our experiments. (For titration data, calculation of buffer intensities, and estimates of corresponding pH changes during reaction of CCl_4, see Supporting Information).

Goethite. Goethite (α-FeOOH) (17 ± 1 m^2/g BET-surface, determined by N_2 adsorption with Sorptomatic 1990, Fisons Instruments) was purchased from Bayer (Bayferrox 910, Standard 86). Tetrachloromethane (Fluka), dichloromethane (Fluka), chloroform (Aldrich), and trichloroethene (Aldrich) were of the greatest available purity ($\geq$99%) and were used as received. Methanol-free CCl_4 spike solutions were prepared by adding 3.5 μL of pure liquid CCl_4 (>99.5%, Fluka) to 110 mL anoxic water (3 h purged with Ar) and stirred for at least 24 h prior to transfer into an anoxic glovebox.

Fe(II) Stock Solutions. Fe(II) stock solutions (0.5 M, pH 5) were prepared by adding 3.63 g (0.065 mol) iron powder (Merck) to 100 mL of a 1.00 M HCl solution (prepared from 32% HCl p.a., Merck) that had been purged with Ar for 1 h. The mixture was heated to 80 °C under slow stirring for 2 h, until most of the powder had dissolved and visible hydrogen evolution ceased. The mixture was subsequently transferred into a glovebox and was filtered through a 0.2-μm PTFE filter to remove excess iron powder. The exact Fe(II) concentration was determined photometrically after complexation with phenanthroline (*32*).

Washing Procedure. To remove traces of organic residues, the glassware used in experiments for formate analysis was (1) soaked in ethanol for several hours, (2) rinsed with deionized water, (3) soaked in 1.5 M HNO_3 for several hours, and (4) rinsed six times with deionized water immediately before use.

Preparation of Goethite/Fe(II) Suspensions. An amount of goethite corresponding to 50 m^2/L was suspended three times in deionized water in order to remove adsorbed ions from the surface. The resulting suspension was sparged with argon for 4 h and subsequently transferred into an anoxic glovebox with external regenerator (Vaccum Atmospheres Corp.) at an oxygen level of ≤0.5 ppm O_2 as monitored by an oxygen sensor (PBI Dansensor, Module ISM-3). There, the pH (initially ∼5) was adjusted with 0.1 M NaOH (Titrisol, Merck) to pH = 7.0. $FeCl_2$ solution was added, and the pH was adjusted again until the desired conditions were obtained (generally 1 mM Fe(II) in solution at pH 7). If necessary, pH and Fe(II) were readjusted after an equilibration time of 48 h. (Sorption of Fe(II) to glassware was found to be negligible.) Two additional sets of experiments were conducted at different conditions: One assay contained 3% (vol) of perdeuterated 2-propanol (Aldrich); the other, only 0.45 mM Fe(II) total (all sorbed to goethite) at a pH of 8.

Iron(II) Porphyrin. Iron(II) porphyrin (*meso*-tetrakis(*N*-Methylpyridyl)iron(II) porphyrin) was prepared from *meso*-tetrakis(*N*-methylpyridyl) iron(III) porphyrin kindly provided by Buschmann (*16*) according to the following method from Wade and Castro (*33*): 13 g of iron powder (>99.5%, Merck) was treated with 1 N HCl for 1 h, transferred into the glovebox, and washed three times with anoxic water. The iron was then added to 0.25 L of 0.5 mM iron(III) porphyrin, and the mixture was shaken for 15 min and subsequently filtered through a 0.2 μM PTFE filter (BGB Analytik). During reduction, the color of the solution changed from green to red, as verified by UV−vis spectroscopy (see Figure S1 in the Supporting Information). In isotope fractionation experiments, the iron(II) porphyrin concentration was adjusted to 150 μM, and 200 μM 4-morpholinopropanesulfonic acid (MOPS, Fluka) was added as buffer at pH 7.

Polysulfide Solutions. Polysulfide solutions were prepared by mixing 49 g (0.2 mol) of $Na_2S{\cdot}H_2O$ (p.a., 32−38% S, Fluka) with 50 g of sulfur powder in 1 L of deionized anoxic water for 2 months (pH 9) (*34*). In isotope fractionation experiments, the polysulfide concentration was adjusted to 40 mM total S(-II), at pH 8.3.

Transformation Experiments of CCl_4. Experiments were set up in the glovebox. For each experiment, 18 replicates were prepared in parallel by transferring 49 g (96 g) of the stirred suspension into 57-mL (115 mL) serum vials. (Values in parentheses describe the setup in isotope fractionation experiments.) Then freshly prepared CCl_4 spike solution was added to yield an initial concentration of 40−50 μM in the product study and 10 μM in the isotope fractionation experiments. The vials were closed with Viton stoppers, taken out of the glovebox, and agitated on a horizontal shaker at 25 °C/140 rpm in the dark until they were sacrificed for analysis. Experiments to study the conversion of CO to formate were set up at pH 7 in 57-mL vials, with (a) 10 mL of goethite/Fe(II) suspension and (b) 10 mL water. Outside the glovebox, the headspace was filled with pure CO gas via a cannula through the Viton septum, corresponding to a concentration of CO in solution of ∼1 mM.

For sampling in the product study, first two 1-mL aliquots of gas were taken from the headspace of the vials by piercing the Viton stopper with a gastight syringe (A2, 1 mL, 0.29 × 0.12 × 2 in., VICI AG) with side-port taper, under simultaneous introduction of 2 × 1 mL of water with a second syringe. These gas samples were subsequently analyzed for CO. Then 7 mL of liquid was withdrawn, to which 300 μL of 0.1 M NaOH was added in order to precipitate Fe(II). This sample was filtered with a 0.2-μm PTFE filter and stored at −20 °C until analysis for formate. Finally, 8 mL diethyl ether (Merck) containing 10 μM trichloroethene as internal standard was added to the remaining suspension. Extraction took place on a reciprocating shaker for 10 min, and 3 × 0.8-mL aliquots of extracts were taken for analysis of chlorinated hydrocarbons.

In isotope fractionation experiments, 10 mL of diethyl ether containing 9 μM benzene (>99.5%, Fluka) as internal standard was added into the headspace of the reaction vials, followed by extraction for 10 min in a reciprocating shaker. Then the cannula of a 1-mL Hamilton glass syringe without piston was bored through the Viton stopper. The ether phase (∼1 mL remained after equilibration) was forced into the glass tube of the syringe by injecting water into the reaction vial through a second cannula; 3 × 200 μL of the ether extract was taken for analysis by GC−C-IRMS.

Analytical Methods. For all analytical methods, external standards were prepared in exactly the same way as the samples. Standards for chlorinated alkanes were set up in serum vials with goethite suspensions (but without Fe(II)), and they were extracted according to the same procedures. Formate standards were set up in goethite/Fe(II) suspensions, which were filtered after addition of NaOH. They had to be prepared daily, because nearly complete disappearance of formate was observed in the goethite/Fe(II) standards at room temperature within a week (see discussion below). CO standards were prepared by mixing varying volumes of a 900 ppm standard with air.

CO Analysis. CO was determined on a gas chromatograph equipped with a thermal conductivity detector (GC-TCD, Shimadzu GC-8A) and a packed column (molecular sieve 8 Å 80/100, Brechbühler, Switzerland). Helium (99.999%) was used as carrier gas at 25 mL/min, the oven temperature was isothermal at 80 °C, injector and detector temperatures were at 150 °C, and the detector current was set at 140 mA. The detection limit of the method was ∼150 ppm.

Formate Analysis. Formate was quantified after enzymatic reaction by measuring the production of NADH photometrically at 339 nm according to a procedure modified from Schaller and Triebig (*35*). A mixture of 0.5 mL of a β-NAD solution (20 mM), 1 mL of phosphate buffer (0.15 M, pH 7.5), and 1.5 mL of sample solution was prepared in a polystyrene vial (Semadeni, all chemicals from Fluka). The photometric absorption of the solution was measured at 339 nm in a quartz precision cuvette (Suprasil, Hellma, 5-cm length). The solution was subsequently transferred back into the polystyrene vial, where 10 μL of formate dehydrogenase solution was added (formate dehydrogenase *Pseudomonas* spec., recombinant mutant to 79900 from *E. coli*; ∼175 U/mL, Fluka Biochemicals, 75274). After an incubation time of 30−60 min at room temperature, the mixture was transferred to the quartz cuvette, which had been cleaned by rinsing twice with deionized water, and the absorption was measured again. The difference between absorption before and after incubation with formate dehydrogenase was used for quantification. The detection limit of this method was ∼2 μM formate (sample concentration in experiment).

Quantification of Volatile Halogenated Compounds. CCl_4 and $CHCl_3$, as well as $CDCl_3$, were quantified on a GC/MS (GC Fisons 8000 Series, autosampler Fisons AS 800, quadrupole MS Fisons MD 800) equipped with a 60 m × 0.32 mm Stabilwax fused-silica column (film thickness 1 μm) and a 8 m × 0.53 mm deactivated guard column. On-column injection was used to introduce 1 μL of sample into the column. The temperature program was 40 °C (2 min), ramp 8 °C/min to 130 °C (0 min), ramp 30 °C/min to 200 °C (5 min). Quantification was carried out in the single ion monitoring mode, for CCl_4 at $m/z = 84, 123$, for $CHCl_3$ at $m/z = 47, 87$, and for $CDCl_3$ at $m/z = 88$. The detection limit of this method was ∼0.1 μM.

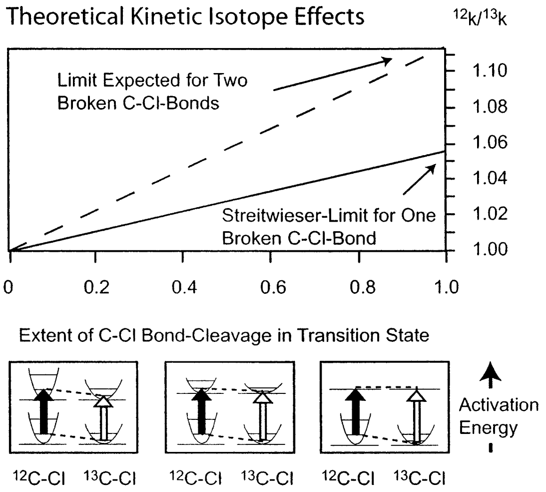

FIGURE 1. Theoretical dependence of the kinetic carbon isotope effect, $^{12}k/^{13}k$, on the extent of bond cleavage in the transition state, for one (solid line) and two broken bonds (dashed line). Small arrow diagrams: activation energies of isotopic bonds in a reactant-like transition state (left), a symmetric transition state (center) and a product-like transition state (right). Note that the difference between the activation energies for isotopic bonds (arrows) becomes larger for later transition states.

GC-C–IRMS Analysis. Concentrations and isotope ratios in isotope fractionation experiments were determined on a GC-C–IRMS (gas chromatograph with combustion unit and isotope ratio mass spectrometer, Finnigan MAT delta$^{\text{plus}}$XL), with a Combi Pal autosampler (CTC Analytics) and a 60 m × 0.32 mm Rtx-VMS column (Restek, Bellefonte, PA). On-column injection was used to introduce 1 μL of sample into the column. The temperature program was 40 °C (2 min), 8 °C/min, 100 °C (5 min), 20 °C/min, 210 °C (8 min). All measurements were run in triplicate (three samples from the extract of the same reaction vial). δ^{13}C values for CCl_4 were automatically determined relative to a CO_2 reference gas. Concentrations of CCl_4 were determined by the peak area ratio of CCl_4 and the internal standard benzene using IRMS data. This yielded calibrations with R^2 of 0.998 (five calibration standards, Fe(II)porphyrin, and polysulfide) and 0.996 (four calibration standards, goethite/Fe(II)), respectively. The goethite used contained trace contaminations of ethyl acetate, which could not be completely baseline-separated from the analyte peak of CCl_4. Their influence on δ^{13}C values of CCl_4 was corrected for by an empirical function obtained from the calibration standards

$$\delta^{13}\mathrm{C}_{\text{measured}} - \delta^{13}\mathrm{C}_{\text{true}} = \frac{1}{2}(-2.3153\ \ln(\mathrm{I}^{44}) + 18.439)$$

where I^{44} is the intensity of the ion beam at the mass 44. The uncertainty of this correction is reflected in a larger error in the goethite/Fe(II) system compared to experiments with Fe(II) porphyrin and polysulfide. Likewise, impurities of tetrahydrofuran in the diethyl ether coeluted with $CHCl_3$. δ^{13}C data for this compound could therefore not be obtained. Kinetic isotope effects were calculated from concentrations and δ^{13}C values of the substrate CCl_4 according to the Rayleigh equation [(*36*), see Figure 3 and S3 in the Supporting Information], with progression of experimental errors in the *x* and *y* directions using the software Lin2d (*37*). The total experimental error, however, is likely to be overestimated by this method so that the errors reported for the resulting enrichment factors describe a confidence interval of >95%.

Theoretical Background. Kinetic isotope fractionation can be expressed by the fractionation factor α or the enrichment factor ($\epsilon = \alpha - 1$) evaluated according to the Rayleigh equation (*36*),

$$\ln \frac{R}{R_0} = \ln\left[f\frac{(1+R_0)}{(1+R)}\right]^{(\alpha-1)} = \ln\left[f\frac{(1+R_0)}{(1+R)}\right]^{\epsilon} \approx \ln f^{\,\epsilon} = \epsilon \ln f \quad (1)$$

with

$$\ln\frac{R}{R_0} = \ln\left[\left(\frac{\delta^{13}\mathrm{C}_{\mathrm{CCl_4}}}{1000}+1\right)/\left(\frac{\delta^{13}\mathrm{C}_{0,\mathrm{CCl_4}}}{1000}+1\right)\right] \quad (2)$$

where R is the isotope ratio ^{13}C/^{12}C in CCl_4 at time *t*, δ^{13}C the isotopic enrichment (in ‰) with respect to the international VPDB standard, and *f* is the fraction of substrate remaining at time *t*, where the subscript index "0" denotes values at time 0 (start of experiment). Because CCl_4 contains only one C atom, all carbon isotopes of the molecule take part in the reaction, and the fractionation factor α obtained by a Rayleigh-type analysis of experimental data is directly equivalent to the inverse kinetic isotope effect at the reactive site

$$\alpha = (^{12}k/^{13}k)^{-1} \quad (3)$$

where ^{12}k and ^{13}k are the rate constants for C–Cl bond cleavage involving ^{12}C and ^{13}C carbon isotopes, respectively.

Such kinetic isotope effects are independent of the absolute value of the activation energy, but strongly influenced by changes in bond strength affecting the vibrational zero-point energy levels in the transition state (TS) (*38*). Reductive dehalogenation of CCl_4 proceeds via a dissociative electron transfer, that is, electron transfer and C–Cl bond cleavage occur simultaneously (*39*). In such a simple bond-breaking process, the kinetic isotope effect, KIE, increases steadily from unity for a very early (= reactant-like) TS to a maximum for a very late (= product-like) TS [see Figure 1 and, e.g., refs *40,41*]. The approximate magnitude of such maximum values can be estimated by calculating Streitwieser limits (*40*), which take into account the contribution of zero-point energy differences to the overall kinetic isotope effect. The calculated value for cleavage of a C–Cl bond (750 cm^{-1}) is $\sim(^{12}k/^{13}k)_{\max} = 1.057$ (*40*). This means that the KIE in reductive cleavage of a *single* C–Cl bond increases from 1.000 for a completely reactant-like TS to ~1.057 for a completely product-like TS and will in most cases adopt intermediate values (see Figure 1). If, however, *two* C–Cl bonds are broken at the same time, then isotopic energy differences will be manifested in *two* weakened bonds in the transition state, and the KIE can be expected to be about twice as large ($1.057^2 = 1.117$ for the maximum KIE and correspondingly lower values for earlier transition states, see Figure 1). A vibrational analysis confirms this conclusion: The reactant CCl_4 (point group T_d) possesses a triply degenerate asymmetric stretching mode (T_2) at 776 cm^{-1} (*42*), whereas the product :CCl_2 (point group C_{2v}) has a nondegenerate asymmetric stretching mode (B_2) at ~750 cm^{-1} (*43*). The two asymmetric stretching modes that are present in the reactant, but not in the product, correspond to the two vibrations that will be weakened and become nonperiodic reaction motions in the transition state if two C–Cl bonds are cleaved simultaneously.

Results and Discussion

Characterization of the Goethite/Fe(II) System with Respect to Fe(II) Sorption. At pH 7.0 the experimentally determined sorption capacity of Fe(II) on goethite was 7–12 μmol/m^2 (or 4.2–7.2 sites/nm^2) for suspensions containing 12.5–100 m^2/L goethite in the presence of 1 mM dissolved Fe(II) (Figure

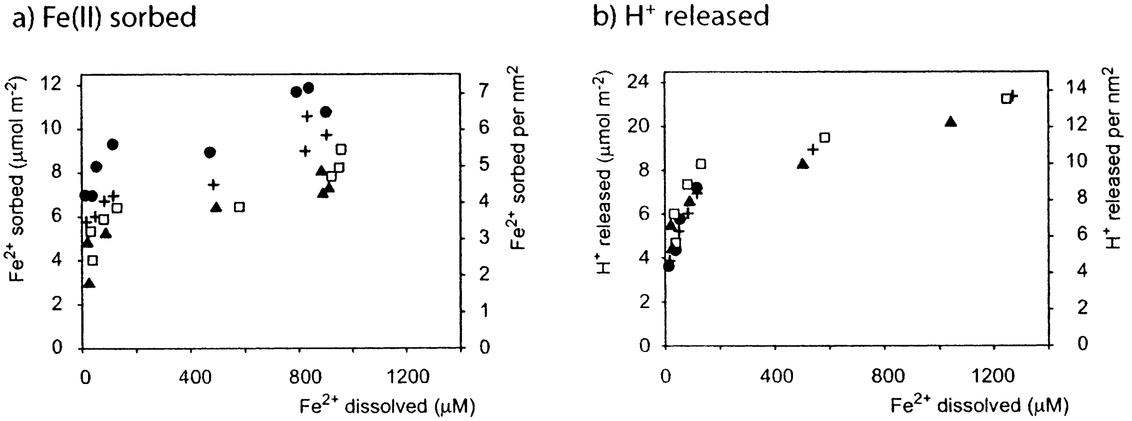

FIGURE 2. (a) Fe(II) sorption isotherms (left) and corresponding "proton release" isotherms (right) at pH 7, calculated from changes in pH values upon Fe(II) addition. ●, 12.5 m^2/L; +, 25 m^2/L; □, 50 m^2/L; ▲, 100 m^2/L mineral loading.

2a). The observed sorption isotherms of Fe(II) revealed several peculiarities:

(1) *Effect of Mineral Loading.* When increasing amounts of goethite were investigated in equilibrium with a constant concentration of 1 mM dissolved Fe(II), the amount of sorbed Fe(II)/m^2 surface area was found to decrease at higher mineral loading. For instance, at a 4 times higher goethite loading, the amount of adsorbed Fe(II) increased only by a factor of 2.3 (Figure 2a). Such a phenomenon has previously been ascribed to particle coagulation and, thus, a decrease of accessible surface area [(*6*); for a more detailed discussion, see Supporting Information].

(2) *Continued Sorption at High Fe(II) Loadings.* After an apparent Fe(II)$_{ads}$ saturation of the goethite surface at 500 μM Fe(II) in solution, uptake of dissolved Fe(II) by goethite continued at higher concentrations of 1 mM Fe(II)$_{aq}$ (Figure 2a). In a previous study, this effect has been ascribed to the onset of surface precipitation processes [(*8*); for a more detailed discussion, see Supporting Information].

(3) *Stoichiometry of Fe(II) Sorption and Proton Release.* From the amount of base that was necessary to adjust the pH after addition and consecutive sorption of Fe(II) to goethite, it was possible to quantify the proton release during the sorption process (see Figure 2b). These calculations made use of the buffer intensity determined beforehand for the goethite/Fe(II) suspensions of this study (see Materials and Methods as well as Supporting Information). Calculated values of $R = (\mathrm{H}^+ \text{ released})/(\mathrm{Fe}^{2+} \text{ sorbed})$ were consistently around 2 (Figure 2a/b), which provides strong experimental evidence for an Fe(II) sorption reaction of the type

$$\text{surface-O}-\text{H} + \mathrm{Fe}^{2+}_{aq} + \mathrm{H_2O} \rightarrow \text{surface-O}-\text{Fe}-\text{OH} + 2\,\mathrm{H}^+ \quad (4)$$

The same surface speciation and sorption stoichiometry has been postulated in previous studies on the basis of surface complexation models [(*25,44,45*); for a more detailed discussion, see Supporting Information]. The buffer effect observed in goethite/Fe(II) suspensions can thus be rationalized in terms of ad- and desorption of Fe(II) at the surface according to eq 4. Moreover, the formation of the neutral surface complexes "surface-O−Fe−OH" suggests that further adsorption of Fe(II) from solution is not prevented by electrostatic repulsion. Thus, high sorption densities may be expected, and possibly even surface precipitation at already slightly alkaline pH and higher concentrations of Fe(II)$_{aq}$.

Effect of Fe(II) Sorption on Dehalogenation Reactivity. Both Amonette et al. (*6*) and Pecher et al. (*8*) found that higher sorption densities of Fe(II) led to an enormous reactivity increase with respect to CCl$_4$ dehalogenation, which was nonlinear in terms of sorbed Fe(II). This elevated reactivity could not be explained by a higher number of isolated S−OFe(II)OH species alone, because otherwise, reaction rates would have depended on their concentration per volume solution, not, as observed, on the sorption density per surface area. Amonette et al. therefore suggested that a simultaneous transfer of two single electrons took place from two adjacent Fe(II) surface sites, thereby leading to a rate law that was second-order with respect to sorbed Fe(II) and first-order with respect to CCl$_4$ (*6*). This explanation, however, must be discarded in our systems for which we present evidence for an initial single-electron transfer (see below). We suggest that an elevated Fe(II) sorption density is instrumental, primarily, in creating a higher concentration of reduced species at the goethite surface. This accumulation may then facilitate the initial transfer of one single electron to CCl$_4$. [An analogous case (single-electron transfer/second-order kinetics) has also been observed in the reduction of CCl$_4$ by Cr(II) (*46*).] Our evidence for surface-Fe(II)OH complexes rather than surface-Fe(II)$^+$ and, thus, the absence of repulsive electrostatic effects corroborates the build-up of such high Fe(II) densities. This accumulation of reduction equivalents could finally correspond to the slow rearrangement of surface bound Fe(II) postulated by Pecher et al. (*8*) and be a first step in the generation of surface precipitates observed by these authors at higher pH.

^{13}C Isotope Fractionation Study To Evaluate the Number of Bonds Broken in the Initial Reaction Step. The carbon kinetic isotope effect for the reductive dehalogenation of CCl$_4$ by goethite/Fe(II) was investigated and compared to the KIE observed for two other model reductants, Fe(II) porphyrin (single-electron transfer, one C−Cl bond broken) and polysulfide (single- and two-electron transfer, one C−Cl bond broken). Evaluation of experimental data according to the Rayleigh equation (Figure 3 and S3) gave kinetic isotope effects of 1.027 for the Fe(II) porphyrin and Fe(II)/goethite systems and 1.023 for the reductant polysulfide, indicative of cleavage of a single C−Cl bond with ~50 and 40% bond weakening in the transition state (see Table 1 and Figure 3c). Although the difference between both values is statistically significant, they are remarkably similar if the wide range of isotope effects, $^{12}k/^{13}k$, is considered that may be expected for this reaction (see Figure 3). Specifically, if two C−Cl bonds were cleaved simultaneously, the kinetic isotope effect would be expected to be twice as pronounced, around 1.046−1.054 (see Figures 1 and 3c), or if both processes took place in parallel, a weighted average would be observed. From the KIE of 1.027 for goethite/Fe(II) it can thus be concluded that generally only one C−Cl bond was broken in the initial step of the reaction with goethite/Fe(II) and that a simultaneous

TABLE 1. Measured and Expected Isotope Effects in Reductive Dehalogenation of CCl$_4$

	ϵ (‰)^a	$\alpha = 1 + \epsilon^a$	$\alpha^{-1} = {}^{12}k/{}^{13}k$
iron(II) porphyrin (single electron transfer, one C−Cl bond broken)	−26.10 ± 1.25	0.973 90 ± 0.001 25	1.0268
polysulfide (partial two electron transfer, one C−Cl bond broken)	−22.22 ± 1.73	0.977 78 ± 0.001 73	1.0227
goethite/Fe(II)	−26.48 ± 2.79	0.973 52 ± 0.002 79	1.0272
expected range for two broken C−Cl bonds			1.046−1.054

^{a} Uncertainties are given as 95% confidence intervals.

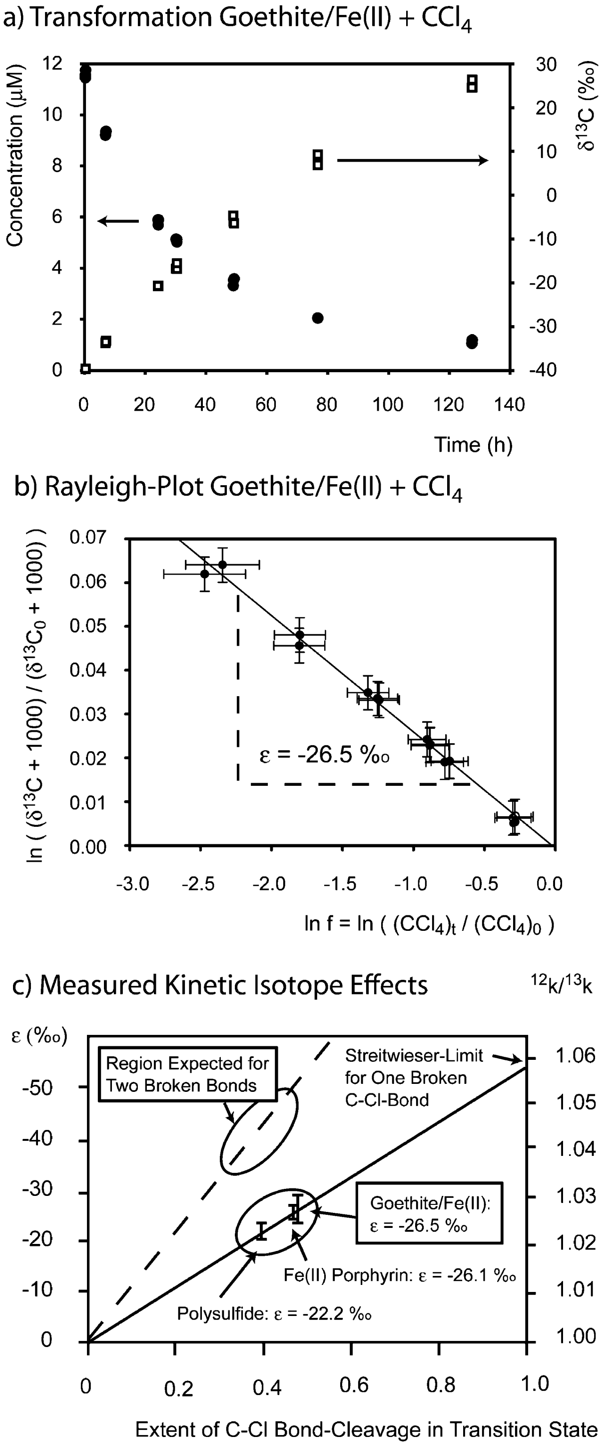

FIGURE 3. (a) Changes in concentration and isotopic signature of CCl$_4$ during reduction by goethite/Fe(II); (b) Evaluation of ϵ according to the Rayleigh equation; (c) Measured and expected isotope effects in reductive dehalogenation of CCl$_4$ with different reductants investigated in this study.

two-electron transfer/two-bond cleavage process must be discarded.

Products in the Dehalogenation of CCl$_4$. Dehalogenation of CCl$_4$ by goethite/Fe(II) at pH 7 produced 33% CHCl$_3$, 20% CO, and up to 40% HCOO$^-$ (see Figure 4a) Other volatile halogenated compounds, such as CH$_2$Cl$_2$, C$_2$Cl$_6$, or C$_2$Cl$_4$, were not detected. In a second experiment, 3 vol % perdeuterated 2-propanol (2-propanol-d_8) was added, which has a weak tertiary C−D bond that facilitates abstraction of D atoms by $^{\bullet}$CCl$_3$ radicals (*16*). [Note that $^{\bullet}$CCl$_3$ radicals are difficult to detect otherwise, as most alternative radical traps, such as nitroxyl radicals, would rapidly be reduced in our system, and analysis by EPR (electron paramegnatic resonance spectroscopy) is not sensitive enough.] The formation of 33% CDCl$_3$ and only 11% CHCl$_3$ (Figure 4b) in the presence of 2-propanol-d_8 indicates (a) that the total yield of chloroform (CHCl$_3$ and CDCl$_3$) was considerably higher due to addition of the $^{\bullet}$D donor, and (b) that a strong competition between $^{\bullet}$H and $^{\bullet}$D donors took place in the system, leading to a much lower yield of CHCl$_3$. The results provide strong evidence that $^{\bullet}$CCl$_3$ radicals were intermediates in the reaction and that, thus, an initial single-electron-transfer took place (Scheme 1).

Formation of CHCl$_3$. Significant fractions of CHCl$_3$ were formed at all experimental conditions studied, despite our attempts to remove organic residues and, thus, possible alternative H$^{\bullet}$ donors from the experimental setup (see Materials and Methods). A possible pathway to explain this result involves the transfer of a second single electron to an initially formed $^{\bullet}$CCl$_3$ radical, leading to a trichloromethyl carbanion (:CCl$_3^-$) (see Scheme 1). In analogy to Scheme 2, :CCl$_3^-$ can either be protonated, thus explaining formation of chloroform, or decompose to dichlorocarbene (*19*), which reacts further to CO (Scheme 3). Results by Pecher et al. (*8*), however, rule out the protonation of :CCl$_3^-$, because no CDCl$_3$ was formed in experiments performed in deuterated water (D$_2$O). This leaves hydrogen (H$^{\bullet}$) transfer to trichloromethyl radicals (Scheme 1) as the most likely process, despite the enforced depletion in organic H$^{\bullet}$ donors. Traces of organic matter at the surface of goethite or present in the deionized water ($f_{oc} \leq 0.1$ mg C/L) supposedly reacted as H$^{\bullet}$ donor with $^{\bullet}$CCl$_3$ radicals. This indicates that minute amounts of organic matter may have affected surface-catalized reductive dehalogenation of CCl$_4$, shifting product distribution toward chloroform.

Formation of CO. Addition of perdeuterated 2-propanol strongly decreased the yield of carbon monoxide (Figure 4a/b). The pathway to CO must, therefore, also involve $^{\bullet}$CCl$_3$ radicals as intermediates, since otherwise, CO formation would not have been affected by the presence of the radical scavenger. The most plausible pathway from $^{\bullet}$CCl$_3$ to CO entails transfer of a second electron, leading to :CCl$_3^-$; then :CCl$_2$ (*19*); HCOCl (*20*); and finally, CO (*21*) (see Schemes 1 and 2). Free trichloromethyl anions (:CCl$_3^-$) in solution, however, must again be discarded on grounds of experiments by Pecher et al. (*8*) with D$_2$O (see above). This indicates that :CCl$_3^-$ may be stabilized in some way, most probably as a short-lived surface complex. Evidence for such a stabilization by complex formation with Fe centers comes from experiments with microsomal cytochrome P-450, where carbenes

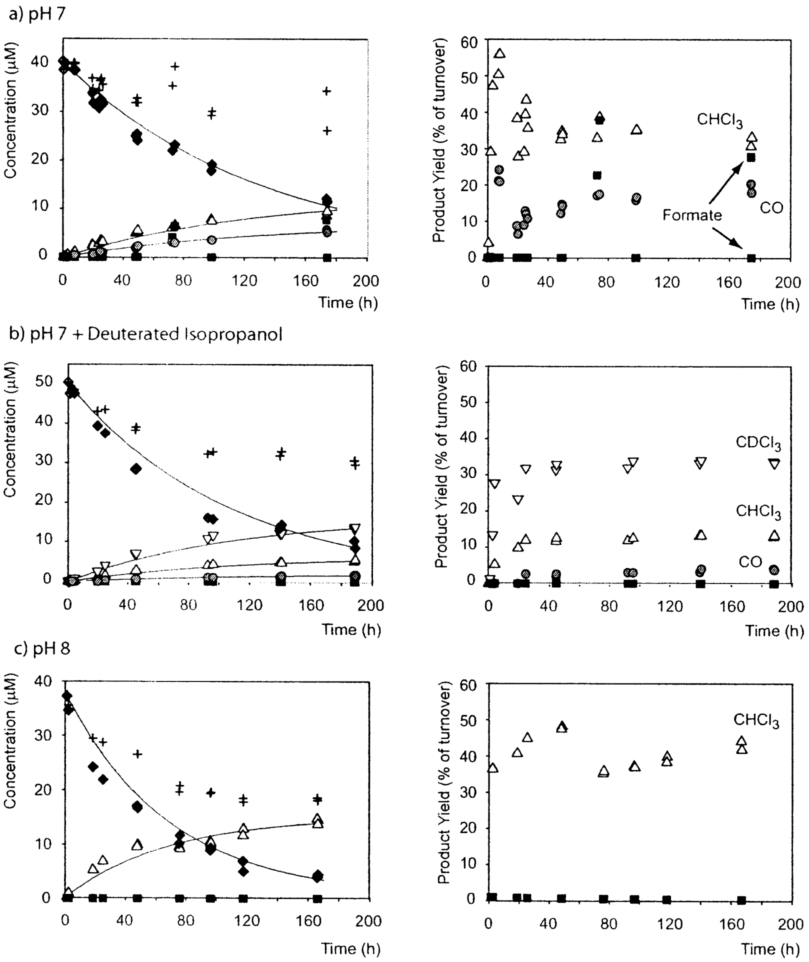

FIGURE 4. Time course and product yield in the reaction of CCl_4 with goethite/Fe(II) (50 m^2/L mineral, 23 °C), (a) at pH 7, (b) at pH 7 with added perdeuterated 2-propanol and (c) at pH 8. ♦, CCl_4; △, $CHCl_3$; ▽, $CDCl_3$; ■, $HCOO^-$; and ●, CO. Crosses indicate molar balance. Lines are exponential fits with pseudo-first-order rate constants (a) 0.0076, (b) 0.0092, and (c) 0.0145 h^{-1} and product yields (a) 33% $CHCl_3$/18% CO, (b) 33% $CDCl_3$/13% $CHCl_3$/4% CO, and (c) 40% $CHCl_3$.

and radicals were found to form iron(II) porphyrin complexes (*47*) (see also ref *48*), as opposed to free radicals, carbanions, and carbenes in solution. One possibility could therefore be the formation of a surface complex of the type

$$[\text{S–Fe(II)}\,{}^{\bullet}\text{CCl}_3 \leftrightarrow \text{S–Fe(III)} - \text{CCl}_3] \xrightarrow{+\,e^-,\,-\,\text{Cl}^-} [\text{S–Fe(II)} = \text{CCl}_2]$$

as a short-lived intermediate in the reaction, where S–Fe(II) denotes surface entities. Formation of CO would thus be possible without transient occurrence of free $:CCl_3^-$ in solution.

Formation of $HCOO^-$. Formate was detected only in some of the reaction vials (see Figure 4), which is consistent with earlier experiments at lower CCl_4 concentrations (data not shown). Contamination can be ruled out, because formate was not found in blanks prepared according to the general strict washing protocol. On the contrary, $HCOO^-$ often disappeared in calibration standards (identical in composition to the reaction vials) with a half-life of 3–4 days. It is therefore likely that formate was produced in all vials to the same extent, but disappeared from some of them in a subsequent reaction. Since all vials were set up identically with regard to their chemical content, but were not sterile (owing to their preparation in a glovebox and the fact that mineral suspensions cannot be filter-sterilized), microbial degradation of formate to CO_2 is a likely cause of the disappearance. We hypothesize that a deficit in the mass balance observed is attributable primarily to microbial oxidation of formate to CO_2, because the carbon-based mass balance was essentially complete in cases where $HCOO^-$ was found (see Figure 4a), and other volatile halogenated compounds were not detected. This assumption is corroborated by recent findings that the iron reducing microorganism *Geobacter metalireducens* (GS 15) is able to grow on formate present at low concentrations (*49*). Production of formate cannot be rationalized by hydrolysis of formyl chloride (HCOCl, see Scheme 2) because decomposition of this intermediate leads to CO at circumneutral pH (*21*). Generation of formate by hydrolysis of CO at pH 7 is thermodynamically favorable ($\Delta G_r^\circ = -73.9$ kJ/mol, see Supporting Information), but was found to be very slow in homogeneous solution, with a half-life of 275 years at our experimental conditions ($k = 8 \times 10^{-4}$ L mol^{-1} s^{-1}, (*50*) where $k = d[HCOO^-]/dt = [OH^-]^{-1}[CO]^{-1}$ and species in brackets denote aqueous concentrations). To test for surface catalysis by goethite, CO hydrolysis was measured at pH 7 in pure water and in the presence of goethite/Fe(II). In both experiments, the headspace contained pure carbon monoxide so that the aqueous concentration of CO corresponded to a saturated solution [17.7 ppm or 9.86×10^{-4} M (*51*)]. Formate could be detected neither in batches with pure water nor in controls of goethite without CO, whereas 3.2–4.8 μM formate was formed in the presence of goethite/Fe(II) after 36–67 days (see Figure S4 in the Supporting Information), indicating surface catalysis of CO hydrolysis by goethite/Fe(II). A rough

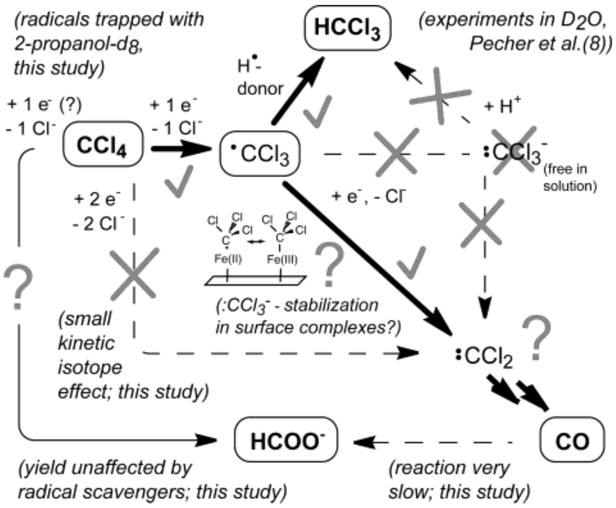

FIGURE 5. Summary of mechanistic evidence obtained for the reaction of CCl_4 with goethite/Fe(II). Compounds in boxes were detected during the reaction. Bold arrows and ticks designate reaction paths for which experimental evidence (written in italic letters) could be obtained, whereas dashed arrows and crosses indicate pathways that must be excluded. Question marks point out hypothesized pathways and intermediates.

estimate of the second-order rate constant ($k = d[HCOO^-]/dt = [OH^-]^{-1}[CO]^{-1} = 1 \times 10^{-2}$ L mol^{-1} s^{-1}) based on these results reveals that the reaction was accelerated by the presence of goethite by a factor of ~10, which is, however, by far not sufficient to explain the amount of formate observed in the dehalogenation experiments of CCl_4. The pathway CO → $HCOO^-$ can therefore be discarded, in accordance with the observation that the radical scavenger 2-propanol-d_8 influenced CO formation but had no effect on the missing mass balance (= product fraction attributable to formate) (see Figure 4b). Formate is therefore likely to be formed by an alternative pathway that does not involve free trichloromethyl radicals as intermediates, possibly because of specific stabilization of intermediates at the surface.

Influence of pH on Product Distribution. Pecher et al. (*8*) observed that higher Fe(II)-surface-site densities at constant pH *decreased* the fraction of $CHCl_3$ formed, whereas an increase of both sorption site density and pH led to *increased* chloroform production. To investigate the influence of pH alone, experiments were conducted at pH 7 and 8, with similar sorption site densities of Fe(II) on goethite. The chloroform yield increased slightly from 33% at pH 7 to ~40% at pH 8 (see Figure 4c). Direct involvement of H^+ in the reaction of CCl_4 to $CHCl_3$ is very unlikely, because H_2O can be expected to be the most important proton donor at circumneutral pH. As discussed above, chloroform is formed by hydrogen ($H^\bullet$) transfer to trichloromethyl radicals rather than by H^+ transfer to trichloromethyl anions. An increase of pH, however, changes the surface chemistry of goethite, leading, for example, to deprotonation of surface hydroxyl groups according to $\equiv S-OH + OH^- \rightarrow \equiv S-O^- + H_2O$. Such processes may affect the formation of surface stabilized intermediates and thus discriminate against alternative pathways in favor of chloroform production. Product formation can, therefore, be expected to be primarily influenced by changes in surface chemistry and only indirectly by pH.

Environmental Significance. By applying various complementary experimental techniques, this study provides new mechanistic information for a better understanding of surface-mediated reductions of chlorinated aliphatic contaminants by Fe(II) (see Figure 5). Our results indicate that the first step in reductive dehalogenation of CCl_4 by surface-bound Fe(II) involves (1) cleavage of only one C−Cl bond and (2) transfer of one electron. This initial reaction was found to generate partly trichloromethyl radicals and to lead partly to formate, possibly via surface-bound intermediates. Consequently, unwanted chloroform was found to be produced mainly in consecutive radical reactions with $H^\bullet$ donors, whereas surface stabilization of short-lived intermediates may play a key role in the alternative formation of benign products. Product formation pathways, therefore, do not primarily depend on the competition between an initial one- and two-electron transfer, but rather on the presence of different radical scavengers and the properties of the mineral surface with respect to stabilization of reaction intermediates. The presence of oxygen and sulfur species can thus lead to completely dehalogenated products in radical reactions (*11*,*16*), whereas even trace amounts of organic matter may result in chloroform formation, as indicated by the results of this study. In addition, specific adsorption of major anions or pH effects may modify the capability of the goethite surface to stabilize short-lived radical intermediates. The key to predicting product formation in reductive dehalogenation of CCl_4 by Fe(II) is, therefore, a profound understanding of the factors that may determine the stabilization of radical intermediates at reactive Fe(II) surface sites. Further research is needed to address this topic, including the effects of coadsorbates, such as inorganic ions and natural organic matter.

Acknowledgments

We thank Lynn Roberts, Klaus Pecher, and Thomas Hofstetter and two anonymous reviewers for helpful comments on the manuscript. This work was funded in part by the Swiss National Science Foundation (Grant No. 21-57171.99), the DOW Foundation Supporting Public Health and Environmental Research Effects (SPHERE) program, and by the Swiss Federal Office for Education and Science (Grant No. BBW 99.0396) as part of the European research project "Protection of Groundwater Resources at Industrially Contaminated Sites" (PURE, EVK1-CT-1999-00030).

Supporting Information Available

Four figures showing (1) UV−vis spectra of Fe(III) and Fe(II) porphyrin, (2) buffer intensity in goethite/Fe(II) suspensions, (3) changes in concentration and isotopic signature of CCl4 during reduction by iron(II) porphyrin and polysulfide (Rayleigh plots), and (4) reaction of CO to formate in suspensions of goethite/Fe(II). In addition, information about the dependence of Fe(II) sorption on mineral loading, characterization of Fe(II) surface complexes, and discussion of possible reactive species; thermodynamic and kinetic data on the conversion of CO to formate. This material is available free of charge via the Internet at http:/pubs.acs.org.

Literature Cited

(1) Arneth, J.-D.; Milde, H.; Kerndorff, H.; Schleyer, R. In *The Landfill, Lecture Notes in Earth Sciences*; Baccini, P., Ed.; Springer-Verlag: Berlin, 1989; Vol. 20 P, p 399.
(2) Christensen, T. H.; Kjeldsen, P.; Albrechtsen, H.-J.; Heron, G.; Nielsen, P. H.; Bjerg, P. L.; Holm, P. E. *Crit. Rev. Environ. Sci. Technol.* **1994**, *24*, 119−202.
(3) Moniel, A.; Rauzy, S. *Toxicol. Environ. Chem.* **1985**, *10*, 315−320.
(4) Plumb, R. H. *Ground Water Mon. Rev.* **1991**, *11*, 157−164.
(5) Matheson, L. J.; Tratnyek, P. G. *Environ. Sci. Technol.* **1994**, *28*, 2045−2053.
(6) Amonette, J.; Workman, D. J.; Kennedy, D. W.; Fruchter, J. S.; Gorbi, Y. A. *Environ. Sci. Technol.* **2000**, *34*, 4606−4613.
(7) Criddle, C. S.; McCarty, P. L. *Environ. Sci. Technol.* **1991**, *25*, 973−978.
(8) Pecher, K.; Haderlein, S. B.; Schwarzenbach, R. P. *Environ. Sci. Technol.* **2002**, *36*, 1734−1741.
(9) Kriegman-King, M. R.; Reinhard, M. *Environ. Sci. Technol.* **1992**, *26*, 2198−2206.

(10) Kriegman-King, M. R.; Reinhard, M. *Environ. Sci. Technol.* **1994**, *28*, 692−700.
(11) Wagner, A. J.; Vecitis, C.; Fairbrother, D. H. *J. Phys. Chem. B* **2002**, *106*, 4432−4440.
(12) Criddle, C. S.; DeWitt, J. T.; Grbic-Galic, D.; McCarty, P. L. *Appl. Environm. Microbiol.* **1990**, *56*, 3240−3246.
(13) Lewis, T. A.; Crawford, R. L. In *Novel Approaches for Bioremediation of Organic Pollution*; Fass, Ed.; Kluwer Academic: New York, 1999; pp 1−11.
(14) Holliger, C.; Schraa, G. *Microbiol. Rev.* **1994**, *15*, 297−305.
(15) Monig, J.; Bahnemann, D.; Asmus, K.-D. *Chem.-Biol. Interact.* **1983**, *47*, 15.
(16) Buschmann, J.; Angst, W.; Schwarzenbach, R. P. *Environ. Sci. Technol.* **1999**, *33*, 1015−1020.
(17) Balko, B. A.; Tratnyek, P. G. *J. Phys. Chem. B* **1998**, *102*, 1459−1465.
(18) Zefirov, N. S.; Makhon'kov, D. I. *Chem. Rev.* **1982**, *82*, 615−624.
(19) Hine, J.; Ehrenson, S. J. *J. Am. Chem. Soc.* **1958**, *80*, 824−830.
(20) Pliego, J. R.; De Almeida, W. B. *J. Phys. Chem.* **1996**, *100*, 12410−12413.
(21) Dowideit, P.; Mertens, R.; von Sonntag, C. *J. Am. Chem. Soc.* **1996**, *118*, 11288−11292.
(22) McCormick, M. L.; Bouwer, E. J.; Adriaens, P. *Environ. Sci. Technol.* **2002**, *36*, 403−410.
(23) Buerge, I. J.; Hug, S. J. *Environ. Sci. Technol.* **1999**, *33*, 4285−4291.
(24) Klausen, J.; Tröber, S. P.; Haderlein, S. B.; Schwarzenbach, R. P. *Environ. Sci. Technol.* **1995**, *29*, 2396−2404.
(25) Liger, E.; Charlet, L.; Van Capellen, P. *Geochim. Cosmochim. Acta* **1999**, *63*, 2939−2955.
(26) Elsner, M.; Schwarzenbach, R. P.; Haderlein, S. B. *Environ. Sci. Technol.* **2004**, *38*, 799−807.
(27) Rügge, K.; Hofstetter, T.; Haderlein, S. B.; Bjerg, P. L.; Knudsen, S.; Zraunig, C.; Mosbaek, H.; Christensen, T. *Environ. Sci. Technol.* **1998**, *32*, 23−31.
(28) Kenneke, J. F.; Weber, E. J. *Environ. Sci. Technol.* **2003**, *37*, 713−720.
(29) Scherer, M. M.; Balko, B. A.; Tratnyek, P. G. In *Kinetics and Mechanisms of Reactions at the Mineral/Water Interface*; Sparks, D. L., Grundl, T., Eds.; ACS Symposium Series; American Chemical Society: Washington, DC, 1999; Vol. 715, Chapter 15, pp 301−320.
(30) Evanko, C. R.; Dzombak, D. A. *J. Colloid Interface Sci.* **1999**, *214*, 189−206.
(31) Kaiser, K.; Guggenberger, G. *Eur. J. Soil Sci.* **2003**, *54*, 219−236.
(32) Fadrus, H.; Maly, J. *Analyst* **1975**, *100*, 549−554.
(33) Wade, R. S.; Castro, C. E. *J. Am. Chem. Soc.* **1973**, *95*, 226−230.
(34) Perlinger, J.; Angst, W.; Schwarzenbach, R. P. *Environ. Sci. Technol.* **1996**, *30*, 3408−3417.
(35) Schaller, K.-H.; Triebig, G. In *Methods of Enzymatic Analysis*; Bergmeier, H. U., Ed.; Verlag Chemie: Weinheim, 1984; Vol. 6, pp 668−672.
(36) Mariotti, A.; Germon, J. C.; Hubert, P.; Kaiser, P.; Letolle, T.; Tardeux, A.; Tardieux, P. *Plant Soil* **1981**, *62*, 413−430.
(37) Graf, T. Ph.D. Dissertation, ETH Zürich, Zürich, 1988; p 134.
(38) Melander, L.; Saunders: W. H. *Reaction Rates of Isotopic Molecules*, 2nd ed.; John Wiley & Sons: New York, 1980.
(39) Costentin, C.; Robert, M.; Saveant, J.-M. *J. Phys. Chem. A* **2000**, *104*, 7492−7501.
(40) Huskey, W. P. In *Enzyme Mechanism from Isotope Effects*; Cook, P. F., Ed.; CRC Press: Boca Raton, Ann Arbour, Boston, London, 1991.
(41) Cook, P. F. *Isot. Environ. Health Stud.* **1998**, *34*, 3−17.
(42) Lide, D. R. *CRC Handbook of Chemistry and Physics*, 76th ed.; CRC Press: Boca Raton, Ann Arbour, Boston, London, 1995.
(43) Cheong, B.-S.; Cho, H.-G. *J. Phys. Chem. A* **1997**, *101*, 7901−7906.
(44) Coughlin, B. R.; Stone, A. T. *Environ. Sci. Technol.* **1995**, *29*, 2445−2455.
(45) Charlet, L.; Silvester, E.; Liger, E. *Chem. Geol.* **1998**, *151*, 85−93.
(46) Castro, C. E.; Kray, W. C. *J. Am. Chem. Soc.* **1966**, *88*, 4447.
(47) Ahr, H. J.; King, L. J.; Nastainczyk, W.; Ullrich, V. *Biochem. Pharmacol.* **1980**, *29*, 2855−2861.
(48) Ziegler, C. J.; Suslick, K. S. *J. Am. Chem. Soc.* **1996**, *118*, 5306−5307.
(49) Straub, K. University of Konstanz, Germany; Personal communication.
(50) Robinson, E. A. *J. Chem. Soc.* **1961**, 1663−1671.
(51) Rettich, T. R.; Battino, R.; Wilhelm, E. *Ber. Bunsen-Ges. Phys. Chem.* **1982**, *86*, 1128−1132.

Received for review July 10, 2003. Revised manuscript received December 12, 2003. Accepted December 19, 2003.

ES034741M